Supplementary Information (SI) for Physical Chemistry Chemical Physics.

Low-Frequency (0-450 cm^{-1}) Dynamics of *n*-Alkyl Cyanide Liquids Studied by Optical Kerr Effect Spectroscopy and Density Functional Theory

Supplementary Information

Dujuan Meng, Sophia Sagala, Edward L. Quitevis*

Department of Chemistry and Biochemistry

Texas Tech University

Lubbock, TX 79409

S1. Results from DFT calculations on *n*-alkyl cyanides.

In this study, DFT calculations were performed to further understand the intermolecular and intramolecular vibrational bands in the reduced spectral densities (RSDs) of the *n*-alkyl cyanides obtained by OHD-RIKES. The calculations were performed using NWChem6.8 program package and the COSMO solvation model.

Table S1. Cartesian coordinates (in Å) of methyl cyanide.

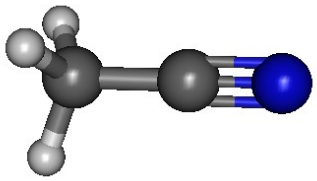

Atom	x	y	z
C	-0.00000000	0.00000000	0.26859443
N	-0.00000000	0.00000000	1.42112723
C	0.00000000	0.00000000	-1.18565193
H	-0.62535376	-0.81442980	-1.55542665
H	1.01799378	-0.13435734	-1.55542665
H	-0.39264002	0.94878715	-1.55542665

Table S2. Cartesian coordinates (in Å) of ethyl cyanide.

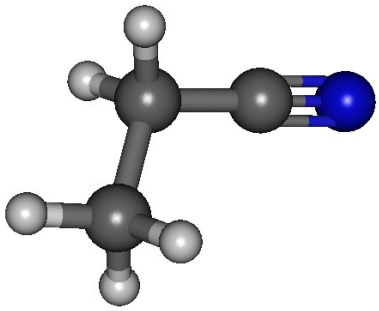

Atom	x	y	z
C	-0.14550140	0.87066093	0.00000000
N	0.25134387	1.95343154	0.00000000
C	-0.63701917	-0.50523708	0.00000000
H	-1.27538922	-0.62814947	0.87926445
C	0.49996708	-1.54211371	0.00000000

H	-1.27538922	-0.62814947	-0.87926445
H	1.12700561	-1.43561193	0.88666983
H	1.12700561	-1.43561193	-0.88666983
H	0.06900212	-2.54439782	0.00000000

Table S3. Cartesian coordinates (in Å) of propyl cyanide staggered-anti.

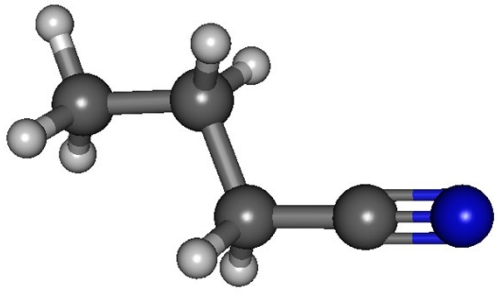

Atom	x	y	z
C	-0.14264097	1.53414231	0.00000000
N	0.24143989	2.62154904	0.00000000
C	-0.61410004	0.15265407	0.00000000
H	-1.24996388	0.01567465	0.88011044
C	0.53800242	-0.87375346	0.00000000
H	-1.24996388	0.01567465	-0.88011044
H	1.16567912	-0.70484321	0.87926936
H	1.16567912	-0.70484321	-0.87926936
C	0.00614709	-2.30757688	0.00000000
H	-0.60780440	-2.50108533	0.88439001
H	0.83088483	-3.02396997	0.00000000
H	-0.60780440	-2.50108533	-0.88439001

Table S4. Cartesian coordinates (in Å) of propyl cyanide staggered-gauche.

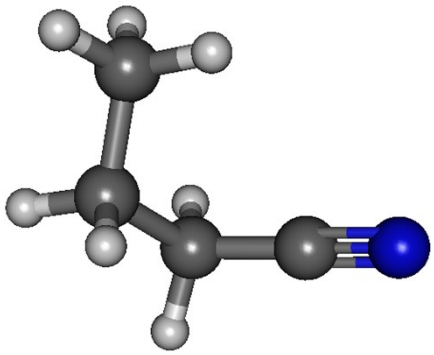

Atom	x	y	z
C	-0.09446835	1.29931752	0.06346522
N	0.60166515	2.20512397	-0.09453125
C	-0.96326858	0.14082258	0.25624507
H	-1.08474563	-0.01399981	1.33327449
C	-0.42278130	-1.14149860	-0.41235663
H	-1.94810648	0.39603000	-0.14489295
C	0.90916160	-1.61982628	0.16733374
H	-0.32930808	-0.96887001	-1.48814130
H	-1.18650120	-1.91216979	-0.27944082
H	1.70064307	-0.88021904	0.01655660
H	1.22605620	-2.54781154	-0.31449434
H	0.82479951	-1.80896238	1.24163892

Table S5. Cartesian coordinates (in Å) of butyl cyanide staggered-anti.

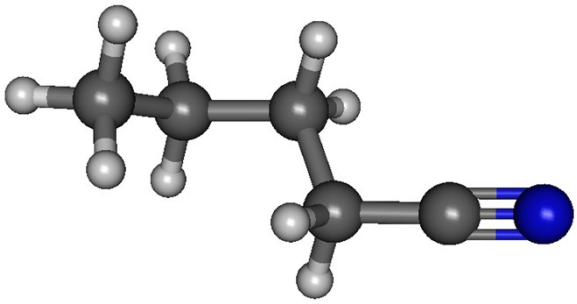

Atom	x	y	z
C	-0.18418860	2.03762512	0.06571567
N	-0.05194847	3.13974731	-0.24729943
C	-0.33759912	0.63861705	0.45091786
H	-0.26129746	0.57885253	1.54184495

C	0.71614748	-0.27694073	-0.20982719
H	-1.35240678	0.33436928	0.18213950
H	1.71036912	0.08863248	0.06059494
H	0.62887935	-0.19532463	-1.29809491
C	0.57735335	-1.74545302	0.21515477
H	0.62460852	-1.80964726	1.30868596
H	1.45262568	-2.28499725	-0.16061860
C	-0.69220969	-2.43967971	-0.29098086
H	-1.60101320	-1.98965671	0.11854883
H	-0.69425082	-3.49523848	-0.00651133
H	-0.75655061	-2.38857495	-1.38245362

Table S6. Cartesian coordinates (in Å) of butyl cyanide staggered-gauche.

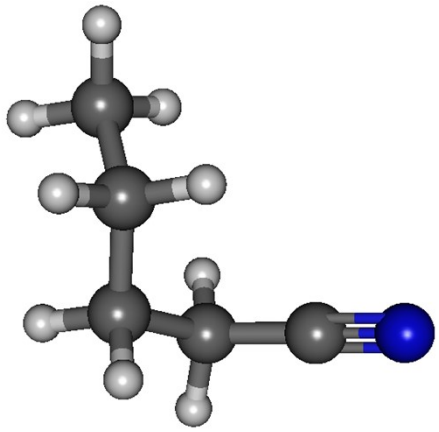

Atom	x	y	z
C	0.07873391	-1.71895021	-0.10998276
N	0.80561779	-2.52783636	0.27403194
C	-0.84430857	-0.68857331	-0.57898563
H	-0.48162777	-0.33063353	-1.54617118
C	-1.00665928	0.47777164	0.42198151
H	-1.81169062	-1.16681625	-0.75583204
C	0.26971703	1.28738327	0.68696253
H	-1.38922142	0.07601889	1.36446175
H	-1.78302522	1.13514361	0.01849040
H	0.05593979	1.99267725	1.49659981
C	0.79101686	2.06167834	-0.52859570
H	1.05393903	0.62142771	1.06530800
H	0.02675149	2.74429941	-0.91348887
H	1.08431020	1.39408614	-1.34365700

H	1.66767848	2.65771288	-0.26132060

Table S7. Cartesian coordinates (in Å) of pentyl cyanide staggered-anti.

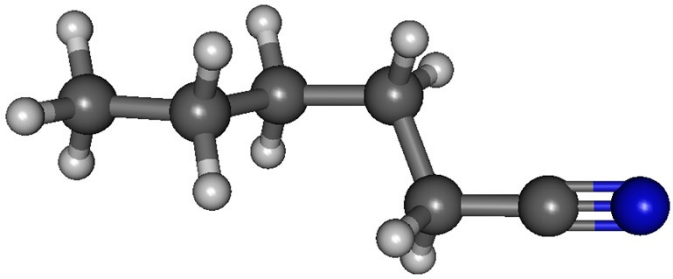

Atom	x	y	z
C	-0.25438739	2.64952157	0.08305936
N	-0.17802979	3.76255438	-0.20915901
C	-0.33406851	1.23651345	0.44012526
H	-0.27413906	1.16033185	1.53101531
C	0.78605671	0.39851182	-0.21624187
H	-1.32444151	0.87896875	0.14659799
H	1.74995122	0.82959737	0.06723637
H	0.70575684	0.48409380	-1.30466088
C	0.74994685	-1.07905347	0.19712361
H	0.76217030	-1.14905910	1.29224458
H	1.67908096	-1.54601089	-0.14852624
C	-0.43549000	-1.88099910	-0.35558823
H	-1.38051165	-1.45985282	0.00460644
C	-0.37211549	-3.36313256	0.02682190
H	-0.45193438	-1.78487176	-1.44785549
H	-0.38814467	-3.48985843	1.11392048
H	0.54593426	-3.82649776	-0.34797063
H	-1.21936149	-3.91710775	-0.38649312

Table S8. Cartesian coordinates (in Å) of pentyl cyanide staggered-gauche.

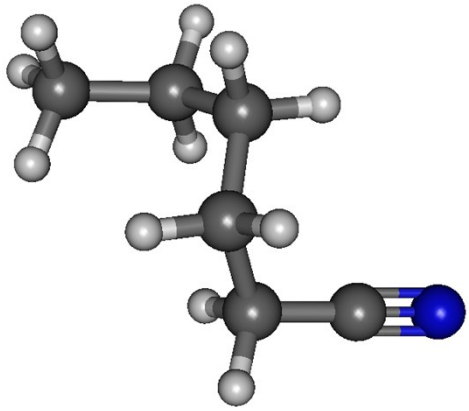

Atom	x	y	z
C	0.06956041	-2.18159625	-0.21788823
N	0.80176933	-3.03652467	0.03348784
C	-0.85816711	-1.09545125	-0.52422990
H	-0.51874105	-0.61825778	-1.44751213
C	-0.98856543	-0.06765951	0.62203772
H	-1.83304006	-1.54346020	-0.73584447
C	0.30546222	0.68255071	0.96953707
H	-1.35524920	-0.58499801	1.51295536
H	-1.77050808	0.63682473	0.32715967
H	0.10286184	1.31058553	1.84470912
C	0.88979679	1.56429010	-0.14659581
H	1.06506258	-0.04175316	1.28555945
C	-0.02420651	2.71404822	-0.58526036
H	1.14777855	0.94842073	-1.01575134
H	1.83678906	1.97984131	0.21428013
H	-0.95260670	2.35015258	-1.03410930
H	0.47244074	3.34696277	-1.32594588
H	-0.29411642	3.34637635	0.26686073

Table S9. Moments of inertia of n-alkyl cyanides from DFT calculations.

Alkyl cyanide	Moments of inertia (a.u)[a]		
	Staggered-anti conformer		
	xx	**yy**	**zz**
Methyl Cyanide	197.391662540769000	-0.000000000000000	-0.000000000000000
	-0.000000000000000	11.291753926899000	0.000000000000000
	-0.000000000000000	0.000000000000000	197.391662540769000
Ethyl Cyanide	382.101437800606000	0.000000022814000	0.000000000000000
	0.000000022814000	64.551396037587000	0.000000000000000
	0.000000000000000	0.000000000000000	424.185107684286000
Propyl Cyanide	792.226965621954000	0.000000101094000	0.000000000000000
	0.000000101094000	76.022461737610000	0.000000000000000
	0.000000000000000	0.000000000000000	834.565189369516000
Butyl Cyanide	1214.098691847860000	-0.000000000000000	-0.000000000000000
	-0.000000000000000	151.884824819469000	0.000000000000000
	-0.000000000000000	0.000000000000000	1273.598797586020000
Pentyl Cyanide	1965.730574717400000	-0.000000000000000	-0.000000000000000
	-0.000000000000000	177.277230215807000	0.000000000000000
	-0.000000000000000	0.000000000000000	2038.211491737100000

[a]1 a.u. = 4.683 x 10^{-48} kg·m^2

Table S10. Internal energy E+ZPE, Gibbs free energy, G, entropic contribution,T·S, for *n*-alkyl cyanides.

Alkyl Cyanides	Energy + ZPE (kcal/mol)	G (kcal/mol)	T·S (kcal/mol)
Methyl Cyanide	-83307.66	-83321.88	17.24
Ethyl Cyanide	-107965.39	-107981.92	20.24
Propyl Cyanide (staggered-anti)	-132624.25	-132642.34	22.54
Propyl Cyanide (staggered-gauche)	-132623.97	-132642.03	22.50
Butyl Cyanide (staggered-anti)	-157281.99	-157301.60	24.78
Butyl Cyanide (staggered-gauche)	-157281.81	-157301.28	24.60
Pentyl Cyanide (staggered-anti)	-181940.44	-181961.86	27.31
Pentyl Cyanide (staggered-gauche)	-181939.49	-181960.60	26.97

Table S11. Raman vibrational frequencies and depolarization ratios for *n*-alkyl cyanides.

Mode	methyl cyanide		ethyl cyanide		propyl cyanide				butyl cyanide				pentyl cyanide			
					anti		gauche		anti		gauche		anti		gauche	
	ν/ cm^{-1}	R_{dp}	ν/ cm^{-1}	R_{dp}	ν/ cm^{-1}	R_{dp}	ν/ cm^{-1}	R_{dp}	ν/ cm^{-1}	R_{dp}	ν/ cm^{-1}	R_{dp}	ν/ cm^{-1}	R_{dp}	ν/ cm^{-1}	R_{dp}
1	396	0.75	219	0.75	95	0.75	100	0.75	62	0.75	61	0.75	43	0.75	34	0.75
2	396	0.75	220	0.75	171	0.75	178	0.74	118	0.75	125	0.75	66	0.75	72	0.75
3	926	0.07	406	0.75	232	0.72	260	0.71	161	0.61	194	0.73	107	0.74	147	0.71
4	1062	0.75	564	0.26	346	0.48	355	0.55	246	0.75	260	0.75	181	0.75	194	0.72
5	1062	0.72	787	0.75	404	0.75	392	0.75	300	0.70	321	0.54	237	0.27	264	0.74
6	1399	0.50	837	0.10	545	0.17	573	0.24	403	0.75	403	0.75	260	0.45	279	0.60
7	1451	0.75	1008	0.36	739	0.75	761	0.08	432	0.22	423	0.72	296	0.06	373	0.75
8	1451	0.75	1086	0.21	871	0.36	842	0.14	546	0.15	580	0.18	403	0.75	400	0.75
9	2353	0.25	1109	0.75	877	0.20	879	0.49	739	0.18	743	0.18	462	0.30	464	0.64
10	3052	0.00	1284	0.75	950	0.41	923	0.48	781	0.13	802	0.11	567	0.19	583	0.17
11	3128	0.75	1341	0.41	1038	0.71	1053	0.75	878	0.41	833	0.24	730	0.74	726	0.37
12	3128	0.75	1403	0.36	1107	0.22	1093	0.65	924	0.56	922	0.64	752	0.41	767	0.13
13			1447	0.68	1126	0.69	1120	0.32	947	0.30	945	0.30	844	0.15	824	0.04
14			1486	0.75	1255	0.72	1245	0.56	983	0.70	980	0.54	860	0.27	874	0.61
15			1486	0.72	1300	0.51	1279	0.33	1070	0.62	1072	0.61	941	0.05	885	0.56
16			2341	0.24	1321	0.74	1347	0.62	1116	0.67	1110	0.65	973	0.34	971	0.14
17			3044	0.01	1372	0.46	1370	0.58	1131	0.57	1125	0.60	986	0.58	978	0.75

18	3047	0.08	1408	0.19	1409	0.26	1226	0.41	1225	0.66	1025	0.32	1014	0.62
19	3082	0.75	1444	0.70	1444	0.64	1274	0.57	1253	0.26	1073	0.73	1077	0.65
20	3117	0.75	1474	0.74	1475	0.74	1308	0.75	1316	0.65	1123	0.74	1121	0.42
21	3119	0.66	1486	0.75	1485	0.75	1325	0.74	1349	0.62	1136	0.33	1123	0.70
22			1495	0.42	1496	0.53	1375	0.51	1379	0.53	1218	0.39	1208	0.68
23			2341	0.25	2339	0.24	1379	0.66	1384	0.60	1266	0.23	1230	0.62
24			3021	0.01	3021	0.01	1411	0.74	1410	0.68	1298	0.60	1282	0.63
25			3031	0.08	3039	0.12	1446	0.74	1452	0.65	1307	0.58	1317	0.49
26			3040	0.04	3041	0.12	1472	0.74	1476	0.74	1330	0.74	1349	0.71
27			3059	0.75	3068	0.63	1484	0.70	1477	0.74	1346	0.73	1364	0.75
28			3076	0.74	3082	0.56	1494	0.75	1492	0.69	1382	0.55	1387	0.66
29			3090	0.60	3091	0.59	1498	0.25	1501	0.75	1397	0.24	1392	0.65
30			3092	0.72	3092	0.59	2340	0.13	2339	0.24	1403	0.68	1405	0.75
31							3011	0.02	3014	0.07	1446	0.71	1452	0.67
32							3017	0.25	3018	0.24	1469	0.73	1475	0.75
33							3027	0.32	3031	0.26	1483	0.67	1483	0.74
34							3041	0.34	3047	0.45	1484	0.75	1483	0.74
35							3047	0.71	3054	0.05	1487	0.66	1490	0.70
36							3067	0.29	3073	0.52	1502	0.74	1504	0.74
37							3079	0.74	3080	0.69	2341	0.25	2338	0.24
38							3083	0.18	3084	0.64	3001	0.13	3007	0.63
39							3090	0.75	3095	0.69	3010	0.07	3011	0.17

40	3014	0.00	3015	0.03
41	3025	0.72	3035	0.44
42	3034	0.06	3038	0.15
43	3042	0.04	3047	0.11
44	3051	0.45	3051	0.05
45	3068	0.57	3074	0.75
46	3075	0.75	3077	0.25
47	3080	0.62	3082	0.71
48	3091	0.58	3091	0.71

R_{dp} = depolarization ratio

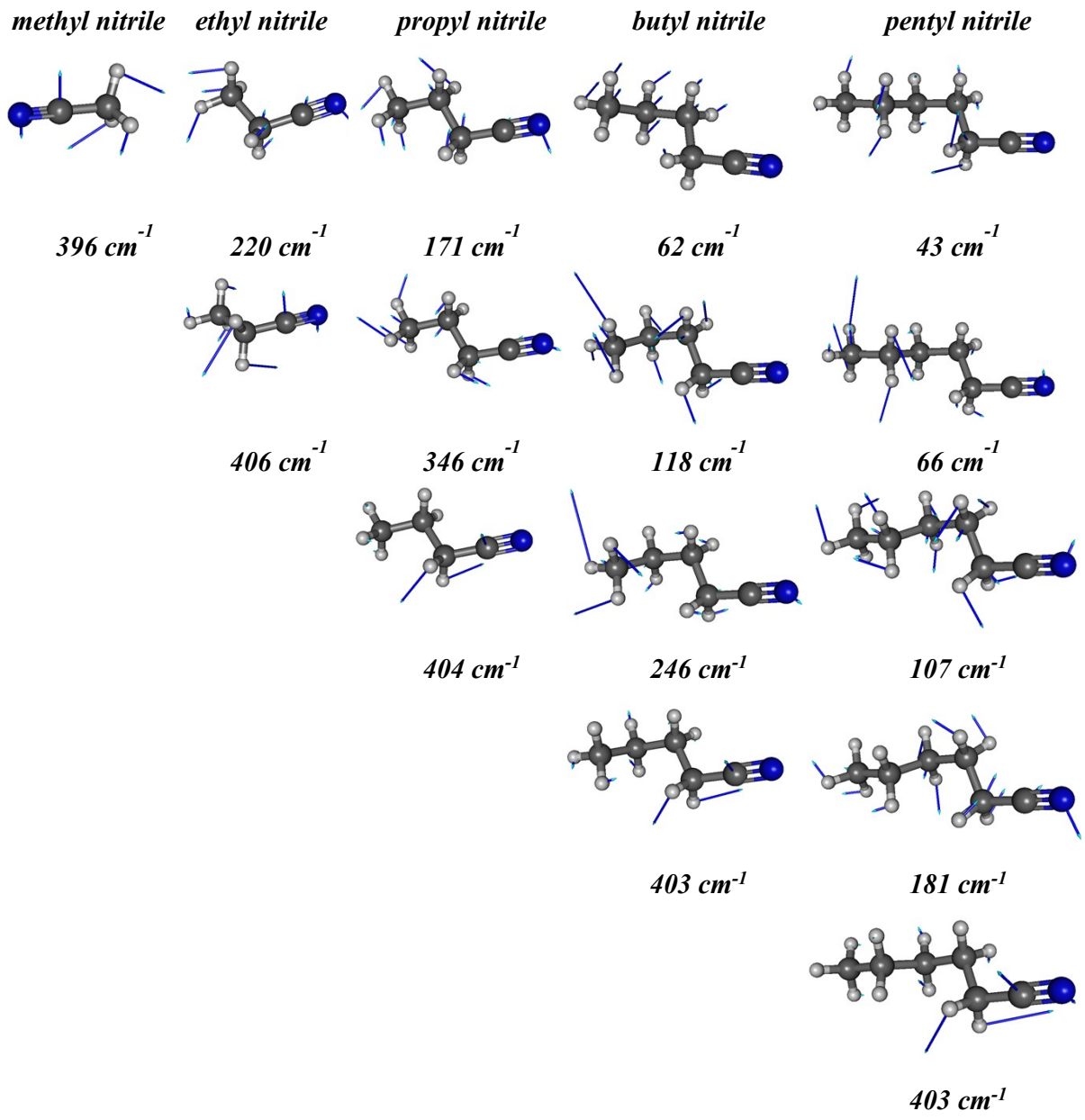

Figure S1. Low frequency (< 405 cm^{-1}) depolarized Raman-active modes of n-alkyl cyanides calculated on the basis of the B3LYP/6311 G(d,p) level of theory. The motions of atoms are shown by the displacement vectors.

S2. OHD-RIKES time-domain responses in the -2-10 ps time range.

The OHD-RIKES time-domain responses of alkyl nitriles (Figure S2) were normalized at the coherent spike (t = 0 ps) and then fit by a biexponential decay function in the 1 to10 ps time range. Figure S3 shows the normalized signals in the -0.5 to 3 ps time range. In this figure, we can see that the intensity of the non-instantaneous part of the OHD-RIKES response increases in going from longer to shorter alkyl chains. The time-domain responses were then fit by a triexponential (eq 1 in the text) in the 1 -10 ps time range yielding a fast decay $\tau_f \equiv \tau_1$ and intermediate decay $\tau_i \equiv \tau_2$, with τ_3 constrained to τ_s from the paper of Zhu et al.[1] The fit parameters are given in Table 1 of the text. The decay times τ_1 and τ_2 are in good agreement with the values in the study of Zhu *et al*.

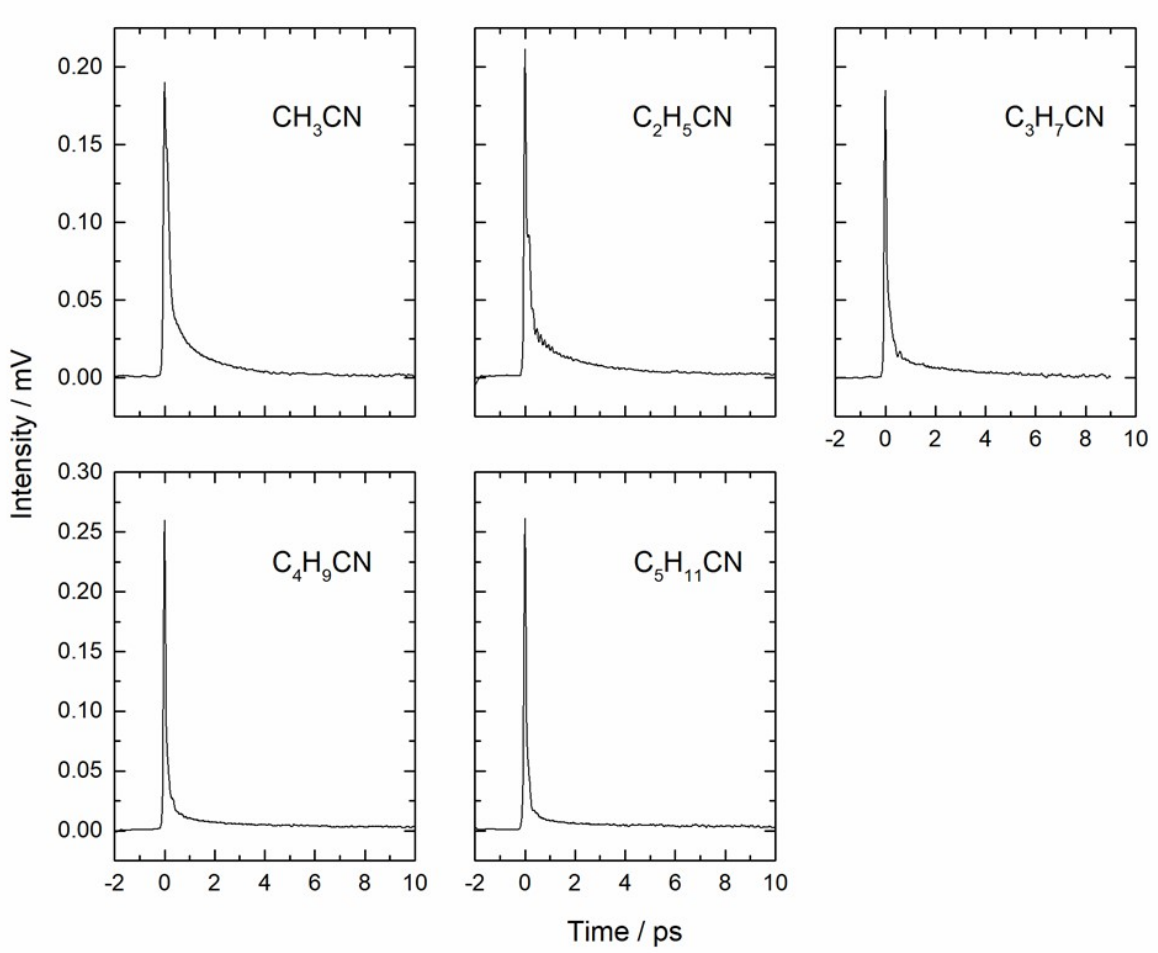

Figure S2. OHD-RIKES time-domain responses in the -2-10 ps time range. For n-propyl cyanide, the signal is shown only up to 9 ps because of the noise at 9-10 ps. But this does not affect the results for the triexponential fits and the RSDs.

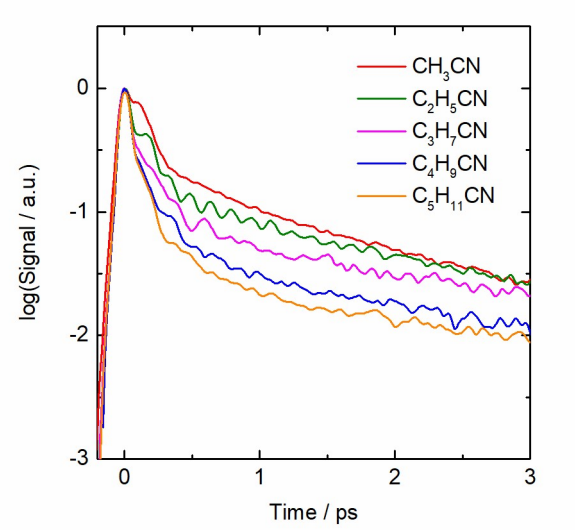

Figure S3. Semilogarithmic plot of the OHD-RIKES time responses of *n*-alkyl cyanides in the -0.5 to 3 ps time range. The responses are normalized at the coherent spike at t = 0 ps.

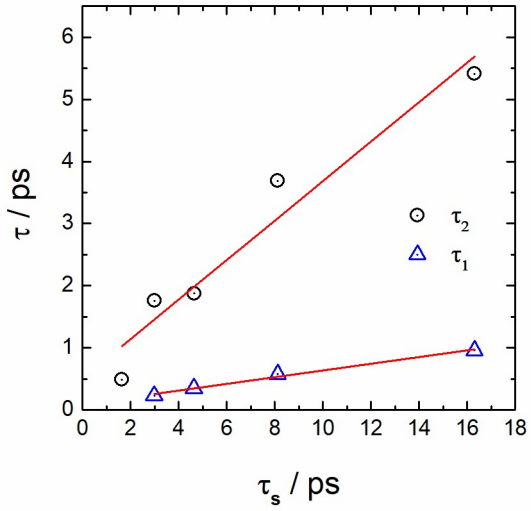

Figure S4. The linear correlation of τ_1 vs. τ_s and τ_2 vs. τ_s. The solid lines are described by the equations $\tau_1 = 0.054 \cdot \tau_s + 0.098$ with $R^2 = 0.9852$, $\tau_2 = 0.318 \cdot \tau_s + 0.506$ with $R^2 = 0.9247$.

Shown in Fig. S4 are linear correlations of τ_1 vs. τ_s and τ_2 vs. τ_s. These correlations indicate that the fast ($\tau_f = \tau_1$) and intermediate ($\tau_i = \tau_2$) processes are dominated by the rate of structural relaxation. Although the nature of the intermediate relaxation time τ_i is not well understood, for most liquids it is correlated to τ_s.[2] One explanation for the intermediate relaxation time τ_i is that it

is associated with spectral diffusion, which arises from fluctuations in the frequencies of the intermolecular modes (motional narrowing).[2, 3]

S3. Multi-component fit parameters**.**

Table S12. Multi-component fit parameters for the RSDs of *n*-alkyl cyanides in the 0 – 250 cm^{-1} region.[a,b]

n-alkyl cyanides	BL			AG1			AG2			AG3			AG4			AG5			χ^2
	A_{BL}	a	ω_{BL}	A_{AG}	ω_{AG}	ε	A_{AG}	ω_{AG}	ε	A_{AG}	ω_{AG}	ε	A_{AG}	ω_{AG}	ε	A_{AG}	ω_{AG}	ε	
CH_3CN	0.051	1.25	18	0.601	62	28	0.180	109	32	-	-	-	-	-	-				0.9996
C_2H_5CN	0.042	1.31	15	0.613	49	26	0.195	91	26	0.365	222	15	-	-	-				0.9930
C_3H_7CN	0.040	1.30	14	0.620	39	24	0.332	81	24	0.239	122	13	0.207	180	27				0.9930
C_4H_9CN	0.018	1.76	9	0.607	35	30	0.396	73	28	0.297	119	26	0.123	210	21				0.9982
$C_5H_{11}CN$	0.035	1.58	7	0.715	28	20	0.625	64	22	0.295	99	21	0.069	143	41	0.071	214	15	0.9998

[a]See eq 7 and 8 in text for definition of fit parameters.

[b]Units of ω_{BL}, ω_{AG}, and ε are in cm^{-1}.

S4. DSE plots - reorientation time vs. η/T

In Figure S5 are shown DSE plots for *n*-alkyl cyanides with the reorientation times taken from study of Zhu et al.[1] The data and fit parameters are given in Table S13.

Table S13. Viscosities and reorientation times for *n*-alkyl cyanide.

Methyl Cyanide			
T / K	η^2 / mPa·s	τ^2 / ps	Slope: 1.118(9)
230	0.795	4.12(5)	
234	0.745	3.83(5)	
254	0.566	2.73(5)	
270	0.462	2.12(5)	
293	0.359	1.64(5)	
307	0.313	1.42(5)	
321	0.276	1.22(5)	
344	0.227	0.98(5)	
Ethyl Cyanide			
T / K	η^4/ mPa·s	τ^1 / ps	
193.3	2.78847	16.9(3)	Slope 1: 1.51(2)
200.6	2.30278	14.3(3)	Slope 2: 0.86(6)
209.3	1.866	11.6(2)	Transition
220.8	1.45015	10.3(2)	temperature:
			224(42) K
221.4	1.43225	10.4(2)	
237.3	1.05474	7.2(1)	
255.4	0.78042	5.1(1)	
272.4	0.61026	4.05(7)	
289	0.49375	3.16(5)	
304.9	0.41199	2.48(8)	
321.2	0.34871	2.24(3)	
337.4	0.30027	1.9(7)	
357.4	0.2544	1.49(6)	
Propyl Cyanide			
T / K	η^4/ mPa·s	τ^1 / ps	
209.5	2.53912	23(1)	Slope 1: 2.04(6)
219.6	2.00573	17.8(7)	Slope 2: 1.65(4)
242.1	1.27306	11.8(9)	Transition
258.1	0.96694	8.9(9)	temperature:

273.9	0.76057	6.0(3)	237.87 K
289.2	0.61807	4.8(2)	
296.7	0.56268	4.5(2)	
313.3	0.46447	3.7(2)	
330	0.39049	3.0(2)	
346	0.33592	2.5(1)	
362	0.29285	2.23(8)	
368	0.27902	2.05(7)	
Butyl Cyanide			
T / K	η^4/ mPa·s	τ^1 / ps	Slope 1: 3.0(2) Slope 2: 2.1(2) Transition temperature: 258.43 K
245.2	1.60136	18(1)	
254	1.3641	16.0(3)	
262.8	1.17431	13.7(6)	
271.6	1.02061	12.8(8)	
280.3	0.89603	10.4(7)	
288.8	0.79492	8.8(4)	
297.5	0.70815	7.4(5)	
306.2	0.63495	7.0(2)	
314.9	0.5727	5.5(2)	
323.7	0.51882	5.5(3)	
332.4	0.47292	4.8(2)	
340.9	0.43396	4.3(2)	
349.5	0.39947	4.1(3)	
357.9	0.36983	3.8(2)	
366.5	0.343	3.5(3)	
Pentyl Cyanide			
T / K	η^4/ mPa·s	τ^1 / ps	Slope 1: 5.4(3) Slope 2: 3.2(5) Transition temperature: 298.54 K
271.1	1.42673	22.1(7)	
288.9	1.05372	16.6(4)	
297.3	0.92606	16(1)	
305.7	0.82024	13.5(7)	
314.1	0.73169	10.9(2)	
323.8	0.64645	8.8(3)	
341.3	0.5271	6.8(2)	

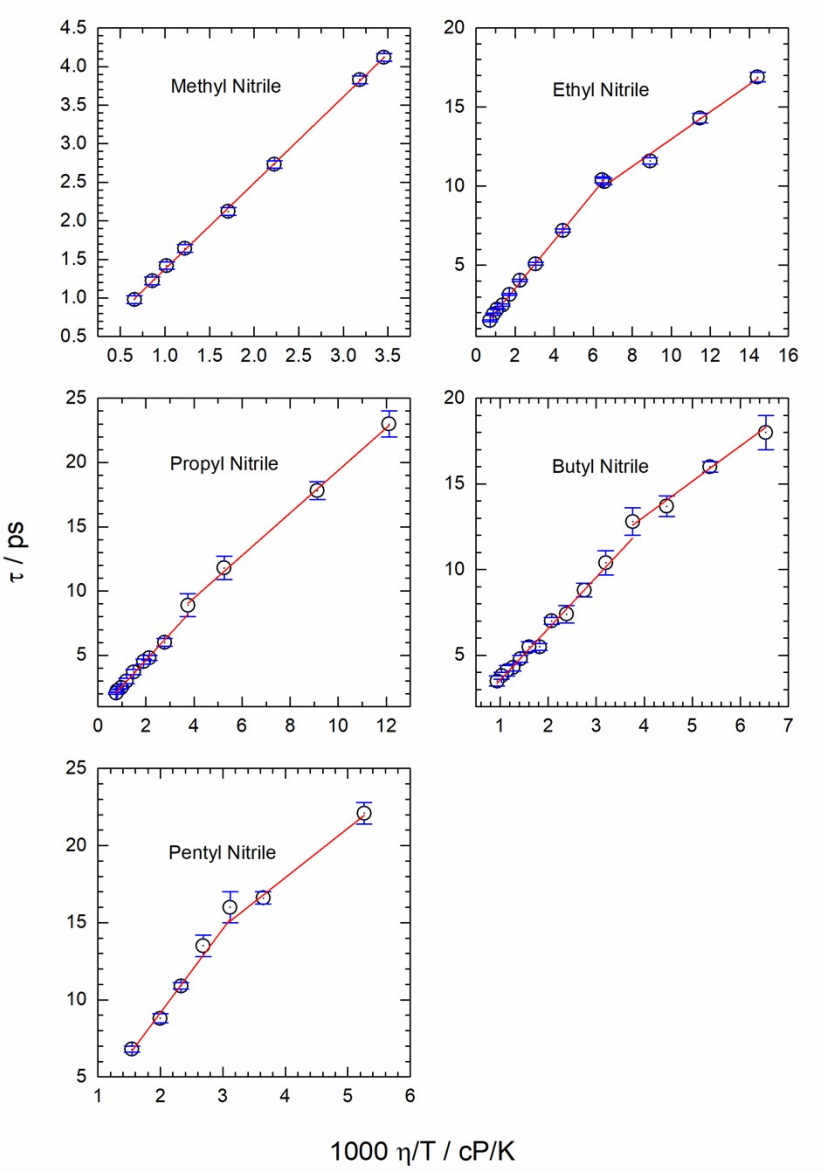

Figure S5. Debye-Stokes-Einstein plots for alkyl cyanides.

S5. Density of *n*-alkyl cyanides

Table S14 gives the literature values[5] of the densities of *n*-alkyl nitriles as a function of temperature, with plots of the density vs. temperature shown in Figure S6 and linear fit parameters listed in Table S15.

Table S14. Densities of *n*-alkyl cyanides.[5]

Temp K	CH_3CN $g \cdot cm^{-3}$	C_2H_5CN $g \cdot cm^{-3}$	C_3H_7CN $g \cdot cm^{-3}$	C_4H_9CN $g \cdot cm^{-3}$	$C_5H_{11}CN$ $g \cdot cm^{-3}$
293.15	0.78181	0.78200	0.79110	0.80010	0.80518
298.15	0.77725	0.77708	0.78690	0.79490	0.8014
303.15	0.77183	0.77194	0.78170	0.79085	0.79711
308.15	0.76628	--	--	--	--
313.15	0.76056	0.76008	0.77157	0.78131	0.78871
318.15	0.75498	--	--	0.80010	--

Table S15. Density Linear Fit Parameters ($\rho = A + B \cdot T$).

Alkyl Nitrile	A $g \cdot cm^{-3}$	B $g \cdot cm^{-3}T^{-1}$	R^2
CH_3CN	1.11014	-1.12×10^{-3}	0.99992
C_2H_5CN	1.105	-1.1×10^{-3}	0.9979
C_3H_7CN	1.0853	-9.86114×10^{-4}	0.99857
C_4H_9CN	1.07257	-9.300557×10^{-4}	0.99883
$C_5H_{11}CN$	1.04818	-8.28343×10^{-4}	0.99911

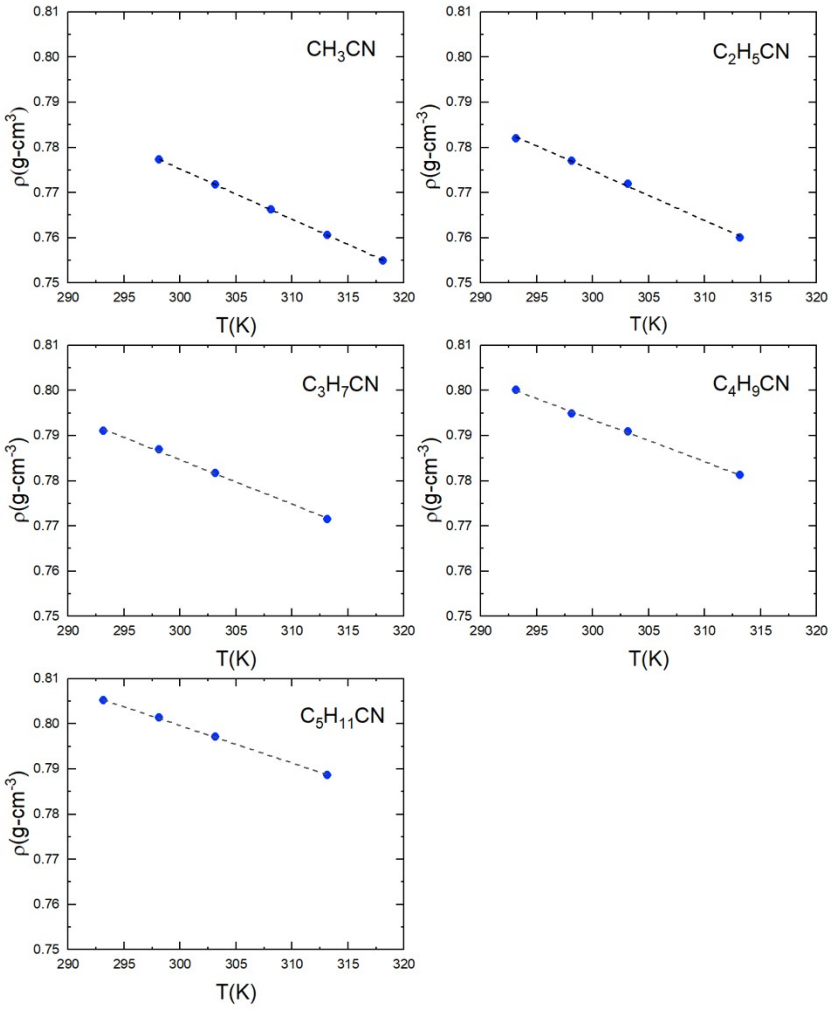

Figure S6. Densities of *n*-alkyl cyanides versus temperature. Dashed lines are fits of $\rho = A + B \cdot T$ to the data (see Table S15 for values fit parameters).

S6. Surface tensions of alkyl nitriles.

Table S16 gives the literature values[6] of the surface tensions of *n*-alkyl nitriles as a function of temperature, with plots of the surface tension vs. temperature shown in Figure S7 and linear fit parameters listed in Table S17.

Table S16. Surface Tension of Alkyl Nitriles.

Temperature (K)	CH_3CN γ(dyn·cm^{-1})	C_2H_5CN γ(dyn·cm^{-1})	C_3H_7CN γ(dyn·cm^{-1})	C_4H_9CN γ(dyn·cm^{-1})	$C_5H_{11}CN$ γ(dyn·cm^{-1})
293.15	29.29	27.32	27.44	27.41	27.83
303.15	28.03	26.17	26.17	26.47	26.92
313.15	26.77	25.02	25.36	25.53	26.01
323.15	25.5	23.86	24.32	24.6	25.10
333.15	24.24	22.71	23.29	23.66	24.20
343.15	--	--	22.25	22.72	23.29
353.15	--	--	21.21	21.78	22.38
363.15	--	--	20.18	20.85	21.48

1 dyn·cm^{-1} = 0.001 Nm^{-1}

Table S17. Surface Tension Linear Fit Parameters ($\gamma = A + B \cdot T$).

Alkyl Nitrile	*A* dyn·cm^{-1}	*B* dyn·cm^{-1}T^{-1}	R^2
CH_3CN	66.317	-0.1263	1
C_2H_5CN	61.122	-0.1153	1
C_3H_7CN	57.366	-0.1024	0.9991
C_4H_9CN	54.888	-0.0937	1
$C_5H_{11}CN$	54.423	-0.0907	1

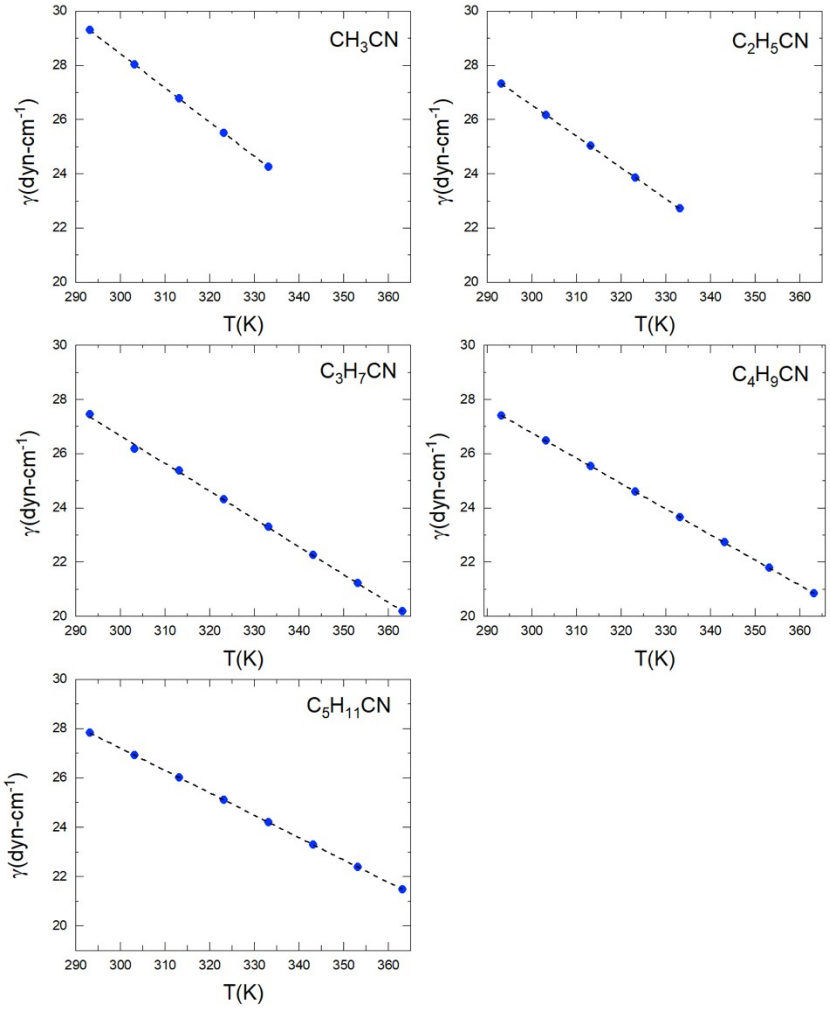

Figure S7. Surface tensions of *n*-alkyl cyanides versus temperature. Dashed lines are fits of $\gamma = A + B \cdot T$ to the data (see Table S17 for values of fit parameters).

S7. Frequency-physical property correlations

Table S18. Parameters for Correlation of Physical Properties to RSD Frequencies.[a-c]

Alkyl Cyanide	M kg-mol^{-1}	ρ kg-m^{-3}	γ N-m^{-1}	$I_{(xx+zz)/2}$ a.u.	I_{perp} 10^{-48}kg-m^2	$(\gamma/M)^{1/2}$ m$^{1/2}$s^{-1}mol$^{1/2}$	$(\gamma/\rho)^{1/2}$ 10^{-3}m$^{3/2}$s^{-1}	$\left(\gamma/I_{perp}\right)^{1/2}$ 10^{21} m$^{1/2}$s^{-1}
CH_3CN	0.041052	781.81	0.02929	197.39	924.38	0.8447	6.121	5.629
C_2H_5CN	0.055079	782.00	0.02732	403.14	1887.90	0.7043	5.911	3.804
C_3H_7CN	0.069106	791.10	0.02744	813.40	3809.15	0.6301	5.889	2.684
C_4H_9CN	0.083133	800.10	0.02741	1243.85	5824.95	0.5742	5.853	2.169
$C_5H_{11}CN$	0.097160	805.18	0.02783	2001.97	9375.23	0.5351	5.879	1.723

[a]Values of ρ(S.I.) and γ(S.I.) at 20 ^{o}C (293.15 K).

[b]Values of $I_{(xx+zz)/2}$ (a.u.) are the average values of I_{xx}(a.u.) and I_{zz}(a.u.) (see Table S9).

[c]I_{perp}(S.I. units) = 4.683 x 10^{-48} x $I_{(xx+zz)/2}$ (a.u.)

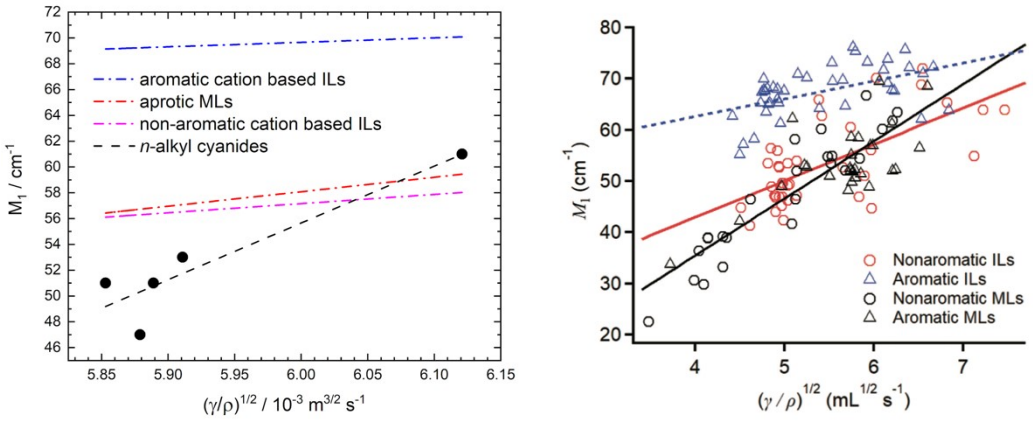

Figure S8. Plots of M_1, the first moment of the intermolecular band, versus $(\gamma/\rho)^{1/2}$, where γ is the surface tension and ρ is the density. The points in the plot on the left correspond to values of M_1 of the *n*-alkyl cyanides obtained in the current study and the dashed line being linear least fit of the points. The dash-dot lines correspond to eq. S1-S3 below. The plot corresponding values of M_1 versus $(\gamma/\rho)^{1/2}$ for a much wider range of liquids was obtained from the literature with permission from ref. 7, copyright, 2020, Chemical Society of Japan.

The dashed-dot lines in the left plot in Fig. S8 were generated using the following equations

$$M_1(cm^{-1}) = 7.11 \times 10^3 \sqrt{\gamma(Nm^{-1})/\rho(kg \cdot m^{-3})} + 14.5 \quad \text{(S1)}$$

$$M_1(cm^{-1}) = 3.51 \times 10^3 \sqrt{\gamma(Nm^{-1})/\rho(kg \cdot m^{-3})} + 48.5 \quad \text{(S2)}$$

$$M_1(cm^{-1}) = 11.2 \times 10^3 \sqrt{\gamma(Nm^{-1})/\rho(kg \cdot m^{-3}} + 9.12 \quad \text{(S3)}$$

where eqns. S1, S2, and S3 are respectively the SI unit equivalent of eqns. 22, 23, and 24 in the study of Shirota *et al*.[7] and correspond, respectively, to linear-least squares fits of the values M_1 for nonaromatic cation based ILs, aromatic cation based ILs, and aprotic molecular liquids (MLs). The left plot shows that the range of values of $(\gamma/\rho)^{1/2}$ for *n*-alkyl cyanides is much narrower than range of values of $(\gamma/\rho)^{1/2}$ in the right plot. The points in the plot of the *n*-alkyl cyanides are lower than the line corresponding either to the aprotic MLs or the nonaromatic cation based ILs. However, if the data for the *n*-alkyl cyanides were included in the plot on right they would lie within the scatter of points corresponding to the aprotic MLs and nonaromatic

based ILs. This suggests that the intermolecular dynamics of *n*-alkyl cyanides are more like that of aprotic MLs or the nonaromatic cation ILs than that of the aromatic cation based ILs. The weaker correlation between M_1 versus $(\gamma/\rho)^{1/2}$ for the aromatic cation based ILs than for the non-aromatic cation based ILs is attributed to the difference in the micro-segregation structures of non-aromatic based ILs and non-aromatic based ILs.[8] The micro-segregation in ILs is characterized by the aggregation of the alkyl chains of the ILs to form nonpolar domains, which are imbedded in a polar ionic network.[9] The degree of heterogeneity as indicated by small wide angle X-ray scattering (SWAXS) data is greater for aromatic cation based ILs than for non-aromatic cation based ILs.[10] This difference is reflected in the Kerr signal being a probe of the ionic region in aromatic cation based ILs and the Kerr signal being a probe of the more homogenous structure of non-aromatic cation based ILs. Aprotic MLs should be largely homogeneous. It is therefore not surprising that the correlation between M_1 versus $(\gamma/\rho)^{1/2}$ for non-aromatic cation based ILs is like the correlation between M_1 versus $(\gamma/\rho)^{1/2}$ for aprotic ILs. One could imagine *n*-alkyl cyanides exhibiting some degree of heterogeneity due to the difference in polarities of the alkyl chains and the cyano groups. However, this difference should not be as great as in the case of ILs and would explain why the correlation between M_1 versus $(\gamma/\rho)^{1/2}$ is more in line with that of aprotic MLs, where micro-segregation is not expected. The strong ion interactions in ILs leads to the self-organizing behavior of ILs, which contributes to micro-segregation. In the case of *n*-alkyl cyanides, dipole-dipole interactions between the cyano groups are not strong enough to lead to the same self-organizing behavior as in ILs. For *n*-alkyl cyanides with long enough alkyl chains micro-segregation may occur. However, to our knowledge, and as confirm by a Web of Science search of the literature, there are no SWAXS

studies of the structure of *n*-alkyl cyanides that would show evidence for micro-segregation in these liquids.

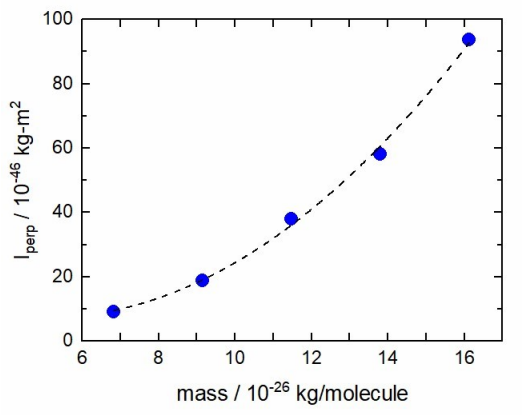

Figure S9. Plot of the moment of inertia I_{perp} versus molar mass M. The dashed line is fit of $I_{perp} = A + B_1 \cdot M + B_2 \cdot M^2$ to the data, with A = 24.80, B_1 = -6.974, B_2 = 24.803, R^2 = 0.998.

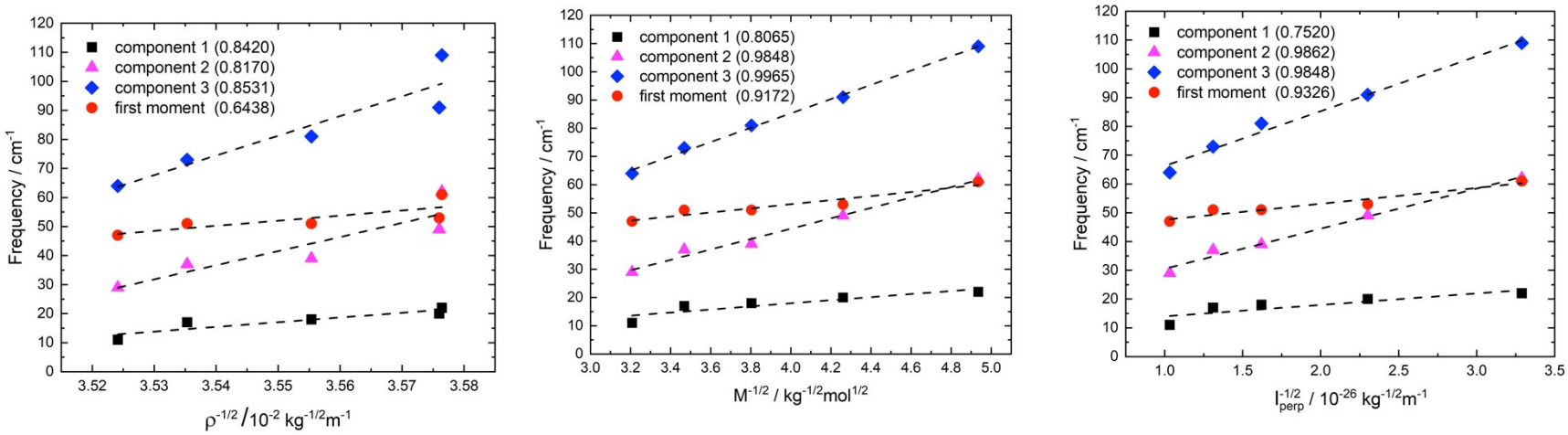

Figure S10. Plots of ω_{pk} for low-, intermediate-, and high-frequency components (components 1-3) and M_1, the first moment of the intermolecular band versus $(1/\rho)^{1/2}$, where ρ is the density (left); versus $(1/M)^{1/2}$, where M is the molar mass (middle); and versus $(1/I_{perp})^{1/2}$, where I_{perp} is the moment of inertia for rotation about axis perpendicular to the long axis of the molecule (staggered-anti conformer) (right). The dashed lines through the points are linear least squares lines with the values of R^2 given in the in the legends.

In Fig. S10 we wanted to determine how correlations between the frequencies of the component bands and intermolecular band and the physical properties of the *n*-alkyl cyanides would change if the surface tension γ was not considered. For the sake of conciseness, we will focus on the correlation between the first spectral moment M_1. The correlation between M_1 and $(\gamma/\rho)^{1/2}$ (Fig. 10) is stronger than the correlation between M_1 and $(1/\rho)^{1/2}$ (Fig S10) ($R^2 = 0.644$ versus $R^2 = 0.851$). In contrast, the correlation between M_1 and $\left(\gamma/I_{perp}\right)^{1/2}$ is not very different than the correlation between M_1 and $\left(1/I_{perp}\right)^{1/2}$ ($R^2 = 0.940$ versus $R^2 = 0.933$). Clearly, the correlation is significantly improved when surface tension is combined with density, but not improved when surface tension is combined with the moment of inertia. However, the correlation between M_1 and $\left(1/I_{perp}\right)^{1/2}$ is considerably greater than between M_1 and $(1/\rho)^{1/2}$ ($R^2 = 0.933$ versus $R^2 = 0.644$), which we found to be case even when surface tension is combined with the moment of inertia. That the correlation between versus M_1 and $(1/M)^{1/2}$is like the correlation between M_1 and $\left(1/I_{perp}\right)^{1/2}$ is consequence of moment of inertia scaling quadratically with the molar mass (Fig. S9). As can be seen in the Fig. S10, these trends also hold for frequencies of the component bands.

References

[1] X. Zhu, R. A. Farrer, Q. Zhong, and J. T. Fourkas, J. Phys-Condens. Mat. 17, S4105 (2005).

[2] B. J. Loughnane, A. Scodinu, R. A. Farrer, J. T. Fourkas, and U. Mohanty, J. Chem. Phys. 111, 2686 (1999).

[3] J. T. Fourkas, in *Ultrafast Infrared and Raman Spectroscopy*, edited by M. D. Fayer (Marcel Dekker, Inc., New York, 2001), pp. 473.

[4] T. K. G. Dabir S. Viswanath, Dasika H. L. Prasad, Nidamarty V. K. Dutt, Kalipatnapu Y. Rani, *Viscosity of Liquids: Theory, Estimation, Experiment, and Data* (Springer, Dordrecht, 2007),

[5] X. H. M. Frenkel, Q. Dong, X. M. Yan, and R. D. Chirico, *Densities of Phenols, Aldehydes, Carboxylic Acids, Amines, Nitrilesand Nitrohydrocarbons* (Springer, New York, 2002), Vol. IV/8I, Thermodynamic Properties of Organic Compounds and their Mixtures, 351-366.

[6] J. J. Jasper, J. Phys. Chem. Ref. Data 1, 841 (1972).

[7] H. Shirota, M. Ando, S. Kakinuma, and K. Takahashi, Bull. Chem. Soc. Jpn. 93, 1520 (2020).

[8] H. Shirota, ChemPhysChem 13, 1638 (2012).

[9] J. N. A. Canongia Lopes, and A. A. H. Padua, J. Phys. Chem. B 110, 3330 (2006).

[10] A. Triolo, O. Russina, B. Fazio, G. A. Appetecchi, M. Carewska, and S. Passerini, J. Chem. Phys. 130, 164521 (2009).